ASCAT SCATTEROMETER WIND QUALITY CONTROL

M. Portabella[(1)], A. Stoffelen[(2)], A. Verhoef[(2)], J. Verspeek [(2)]

[(1)] Unidad de Tecnología Marina – CSIC, Pg. Marítim Barceloneta 37-49, 08003 Barcelona, Spain,
Email: portabella@cmima.csic.es
[(2)] Royal Netherlands Meteorological Institute (KNMI), Postbus 201, 3730 AE De Bilt, The Netherlands,
Emails: stoffele@knmi.nl, verhoefa@knmi.nl, verspeek@knmi.nl

ABSTRACT

The so-called Advanced scatterometer (ASCAT), onboard MetOp-A satellite was successfully launched on October 19 2006. ASCAT derived sea surface wind field observations are well within the mission accuracy requirements. An important part of the Numerical Weather Prediction Satellite Application Facility (NWP-SAF) ASCAT Data Wind Processor (AWDP) is the wind data quality control (QC). This paper shows the implementation of a new QC procedure, based on the wind inversion residual, which significantly improves the effectiveness of the scatterometer wind data QC.

1 INTRODUCTION

The Metop-A satellite was launched on 19 October 2006 and carries the Advanced Scatterometer (ASCAT). The instrument is a real aperture, C band, vertically polarized radar with three fan beam antennas pointing to the left hand side of the sub-satellite track and three fan beam antennas pointing to the right hand side. Scatterometers are known to provide accurate mesoscale (25-50 km resolution) sea surface wind field information used in a wide variety of applications, including Numerical Weather Prediction (NWP) data assimilation, nowcasting, and climate studies. The radar antenna geometry, the measurement noise, as well as non-linearities in the relationship between the backscatter measurements and the wind vector complicate the wind retrieval process. In addition, scatterometers are sensitive to geophysical phenomena other than wind, such as confused sea state, rain, land & ice contamination of the radar footprint. These phenomena can distort the wind signal, leading to poor quality retrieved winds. As such, elimination of poor quality data is a prerequisite for the successful use of scatterometer winds.

An important tool in the interpretation of the ASCAT data is the visualization of triplets of radar backscatter or σ^o measurements (corresponding to the three antenna beams) in the 3-dimensional measurement space. For a given position across the swath, the ASCAT measured triplets are distributed around a well-defined "conical" surface (see Figure1) and hence that the signal largely depends on just two geophysical parameters, i.e., wind speed and direction. Such cone, the so-called Geophysical Model Function (GMF) represents the best fit to the measured triplets and can in turn be used for, e.g., inter-beam calibration [1] or Quality Control (QC) purposes. As previously mentioned, the radar backscatter measurements may be a function of certain geophysical parameters other than wind. As such, it is important to assess the magnitude of the triplet departures from the two-parameter function (i.e., the GMF). A way to investigate such departures is to look at the maximum likelihood estimator (MLE) parameter, which can be interpreted as a measure of the distance between the set of radar measurements (triplets) and the cone surface in a slightly transformed measurement space.

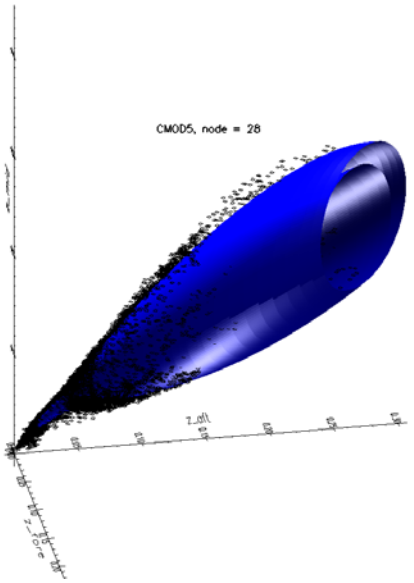

Figure 1. Visualization of the CMOD5.n GMF (blue surface) and the ASCAT triplets (black dots) in 3D measurement space, for Wind Vector Cell (WVC) number 28. The axes represent the fore-, aft- and mid beam backscatter in z-space, i.e., (z_{fore}, z_{aft}, z_{mid}) where $z=(\sigma^o)^{0.625}$ [1].

In general, the triplets lie close to the cone surface (i.e., low MLE values), further validating the two-parameter (i.e., wind vector) GMF. As shown by several QC procedures developed for previous scatterometer missions (e.g., [2]), a large inconsistency with the GMF results in a large MLE, which indicates geophysical conditions other than those modelled by the GMF, such as rain, confused sea state, or ice, and as such, the MLE provides a good indication for the quality of the retrieved winds. However, no work has been done in investigating the correlation between the quality of the retrieved winds and the MLE sign (a sign can be assigned to the distance-to-cone, depending on whether the triplet is located inside or outside the cone surface). In this paper, we propose a QC method, which not only depends on the magnitude of the MLE but also on the sign.

2 MLE SIGN AS A QC INDICATOR

For the first three years of the MetOp-A mission, the ASCAT QC procedure implemented in AWDP was based on the ERS scatterometer QC. The inversion residual or MLE was normalized by the measurement noise (see Portabella and Stoffelen, 2006) and a WVC-dependent factor. A fixed threshold value of this normalized MLE (hereafter referred as MLE), i.e., 18.6, is used in AWDP to discriminate between poor and good quality wind data. As such, a WVC with MLE value below (above) 18.6 is accepted (rejected) in the processing chain. Table 1 summarizes the overall performance of the ASCAT MLE-based QC. The mean vector root-mean-square (VRMS) difference between ASCAT and European Centre for Medium-range Forecasts (ECMWF) model winds is used as a quality indicator. The substantial difference in terms of quality (relative to ECMWF model winds) between accepted and rejected WVCs denotes an effective QC.

QC	Fraction of data (%)	VRMS (m/s)
Accepted	99.6	1.72
Rejected	0.4	4.25

Table 1. Percentage and Mean VRMS difference between ASCAT and ECMWF winds for accepted and rejected data.

Figure 2 shows a schematic illustration of a cross section of the cone surface shown in Figure 1. Note that such cross section is almost perpendicular to the cone, and mainly shows the variation due to wind direction (ø) at approximately constant wind speed. By computing the inner product of **s-m** and **s-o** (see Figure 2), one can straightforwardly determine whether the measurement triplet is inside or outside the cone surface, i.e., the inner product will be positive when the triplet (**o**) is inside the cone and negative when the triplet is outside the cone.

By accounting for a MLE sign, the ASCAT QC threshold (18.6) is applied to the absolute value of the MLE to mimic the old (signless) MLE-based procedure.

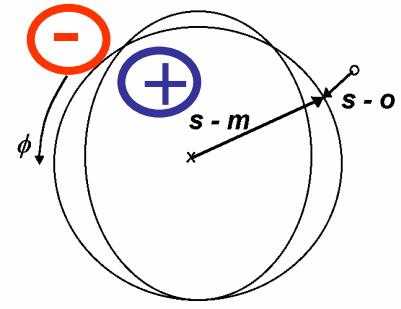

Figure 2. Schematic illustration of a cross section of the CMOD5.n GMF shown in Figure 1.Note that s refers to a point on the cone surface as determined by inversion; m represents the major axis location at this cross section; and o represents the measurement triplet.

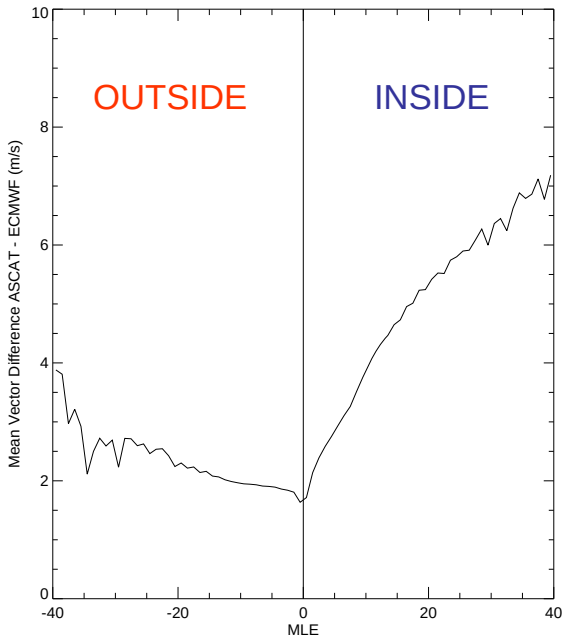

Figure 3. Mean vector root-mean-square (VRMS) difference between ASCAT and ECMWF winds as a function of MLE. Note that negative (positive) values correspond to triplets outside (inside) the cone surface.

To characterize the correlation between the MLE and the quality of retrieved winds, the mean VRMS difference between scatterometer and ECMWF winds is widely used as a quality indicator (e.g., [2]). Figure 3 shows the mean VRMS difference between ASCAT and ECMWF winds as a function of the MLE magnitude and sign. There is a clear distinct behaviour for positive and negative MLEs in terms of data quality. On the one hand, ASCAT winds derived from triplets located inside the cone rapidly decrease in quality as the triplet's distance to the cone surface increases (i.e., see steep increase of VRMS as a function of MLE, for positive MLE values). On the other hand, for triplets lying outside the cone surface, the ASCAT wind quality degradation is generally small regardless of the triplet distance to the cone (see the relatively small slope of the VRMS curve as a function of MLE, for negative MLE values). As such, since fall 2009, the AWDP QC procedure was updated to account for the MLE sign. In particular, the new QC procedure does not reject any wind data from triplets located outside the cone surface (i.e., with negative MLE values). The MLE threshold value is kept the same (18.6), although it is not applied to the absolute value of the MLE but to the MLE value itself.

3 ANALYSIS OF MLE SIGN BASED QC

Figure 4 shows the histogram of relative wind direction (solid) together with the mean (dashed thin) and the standard deviation SD (dashed thick) of the wind speed as a function of the relative wind direction for two different wind sources, i.e., ASCAT (left panels) and ECMWF (right panels), and for accepted (top panels) and rejected (bottom panels) WVCs. The ASCAT wind direction distribution is very similar to that of ECMWF for QC-accepted WVCs, denoting good agreement between both wind sources. However, for rejected WVCs, the ASCAT distribution is substantially different from that of ECMWF. The former has clear artificial (non geophysical) accumulations at certain wind directions (solid curve in bottom left panel). This systematic effect in the direction retrievals is well known in scatterometry and has been reported by several authors (e.g., [3], [4]). It is undesirable and therefore important to remove or at least to mitigate. As such, by detecting such artefacts, the ASCAT QC shows good performance.

The ASCAT mean wind and its SD also show unrealistic peaks (as compared to ECMWF) at certain wind directions for QC-rejected WVCs, denoting again good performance of the QC procedure. However, these same peaks, although reduced, are also seen in the QC-accepted WVCs (dashed thin line in top left panel). Further analysis is required to check whether the mean wind speed peaks can be removed or reduced by using a more constrained QC threshold (lower value than 18.6).

Rain Effects

Rain is known to both attenuate and scatter the microwave signal [5]. Rain drops are small compared to radar wavelengths and cause Rayleigh scattering. As the rain rate increases, the radar sees less and less of the radiation emitted by the surface, and increasingly sees the radiation emitted by the rainy layer that becomes optically thick due to volumetric Rayleigh scattering [6]. The higher the frequency of the radar, the larger is the impact of both effects (rain attenuation and scattering). ASCAT operates at a relatively low frequency (5 GHz) and, as such, the mentioned effects are expected to be small. However, in addition to these effects, there is a "splashing" effect. The roughness of the sea surface is increased because of splashing due to rain drops. This increases the radar backscatter (σ^o) measured, which in turn will affect the quality of wind speed (positive bias due to σ^o increase) and direction (loss of anisotropy in the backscatter signal) retrievals.

Another effect associated with heavy rain is increased wind variability. Convective rain cools the air below and reinforces downdraft near convective cells. These downdrafts often hit the ocean surface and cause outflow over the ocean, leading to variable wind speeds and directions. Such variability within a WVC would increase the isotropy of the radar backscattering at the ocean surface and therefore move the ASCAT triplet inside the cone. Moreover, ECMWF winds do not resolve downdrafts and thus provide relatively poor surface verification (high RMS difference) in such conditions, while the scatterometer winds may be reasonable.

One year (2008) of ASCAT and Tropical Rainfall Measuring Mission's (TRMM) Microwave Imager (TMI) collocations are used to study the effect of rain in ASCAT retrievals and the performance of the QC procedure. Figure 5 shows the histogram of MLE for different rain rate (RR) intervals. There is a clear bias of the MLE distributions towards positive MLE values as RR increases. At RR= 0 mm/hr, the MLE distribution is almost symmetric with respect to the cone surface (almost the same distribution inside and outside the cone). In contrast, at RR above 6 mm/hr, most of the WVC triplets are located inside the cone (positive MLEs), with a substantial amount of triplets very far way from the surface (large positive MLE values). This is an expected effect, since rain tends to produce a loss of anisotropy of the radar signal, therefore projecting the backscatter triplets inside the cone surface.

Figure 6 shows the mean VRMS difference between ASCAT and ECMWF winds as a function of rain rate.

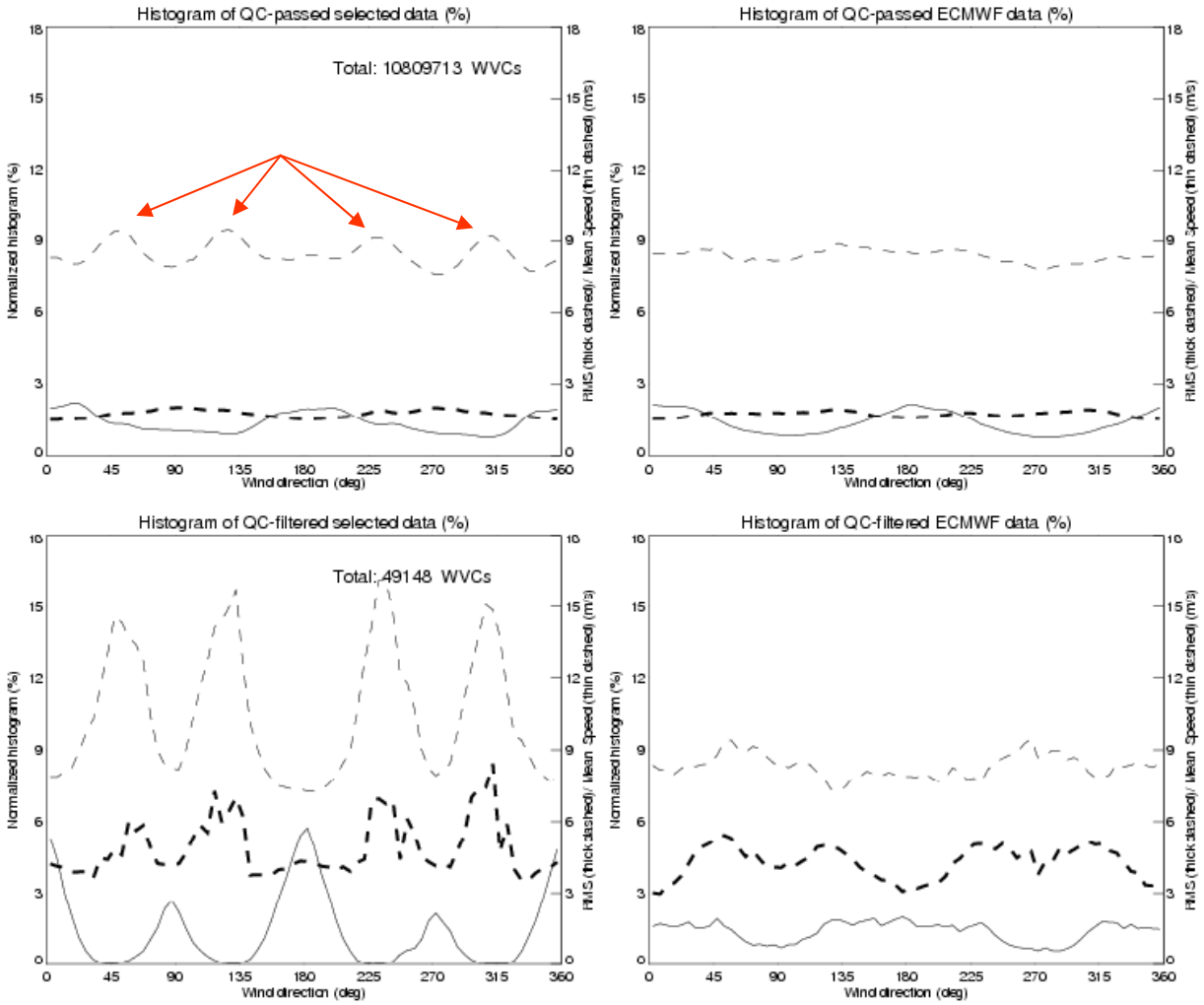

Figure 4. Histogram of wind direction (solid) relative to the ASCAT mid antenna beam (e.g., 0° corresponds to wind blowing towards the mid beam) together with the mean (dashed thin) and the standard deviation SD (dashed thick) of the wind speed as a function of the relative wind direction for two different wind sources, i.e., ASCAT (left panels) and ECMWF (right panels), and for accepted (top panels) and rejected (bottom panels) WVCs by QC. Note that only WVCs with retrieved wind speed above 4 m/s are used.

As expected, there is an increasing degradation of ASCAT derived winds for increasing rain rates. However, the substantial degradation within the first few mm/hr bins (the mean VRMS value is roughly doubled at 3mm/hr as compared to the no-rain value) is beyond the expected (small) rain impact in the C-band backscatter for such (low) rain rates. This increase in VRMS can alternatively be interpreted as an increase of ECMWF wind errors over rainy areas. Since the ASCAT TMI collocations are mostly within the tropics, ECMWF may be missing near-equatorial rain-related effects, such as downbursts and convergence.

Figure 7 shows the wind speed histogram of both ASCAT (a) and ECMWF (b) winds for different TMI-derived RR intervals. There is a clear positive wind speed shift in the ASCAT distributions for increasing RR which is not present in the ECMWF distributions. Although the (ASCAT) positive shift is consistent with the already mentioned rain splashing effect, the latter is expected to be small at such (low) rain rates. Moreover, downbursts and convergence are known to produce an increase in wind speed which is not well resolved by ECMWF (see rain-independent histograms in Figure 7b). However, for RR above 6 mm/hr, the substantial difference between ASCAT and ECMWF wind distributions seems to be well beyond the ECMWF uncertainty for rainy conditions, indicating a noticeable rain impact in the radar backscatter signal at such rain regimes. It is therefore concluded that the ASCAT QC should reject WVCs with RR above 6 mm/hr.

Figure 8 shows an ASCAT retrieved wind field with TMI collocated rain rate values superimposed (a) and the collocated ECMWF wind field (b). Note that the ASCAT wind convergence area under light rain around 14°N and 125°W is not present in the ECMWF wind field. Moreover, ASCAT winds are somewhat higher than ECMWF winds in that area. A more thorough analysis is needed to better characterize, for light rain conditions, the rain impact on scatterometer winds and on ECMWF wind uncertainty.

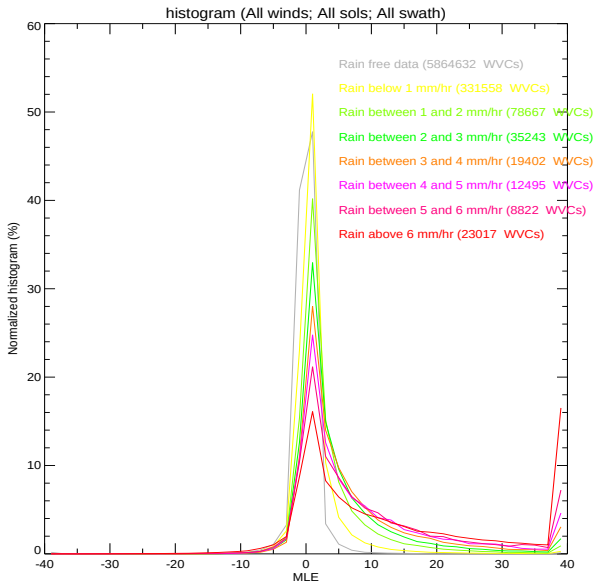

Figure 5. MLE histogram for different rain rate (RR) intervals. Note that every colored line corresponds to a different RR interval (see legend). The number of WVCs for each histogram is also provided in the legend.

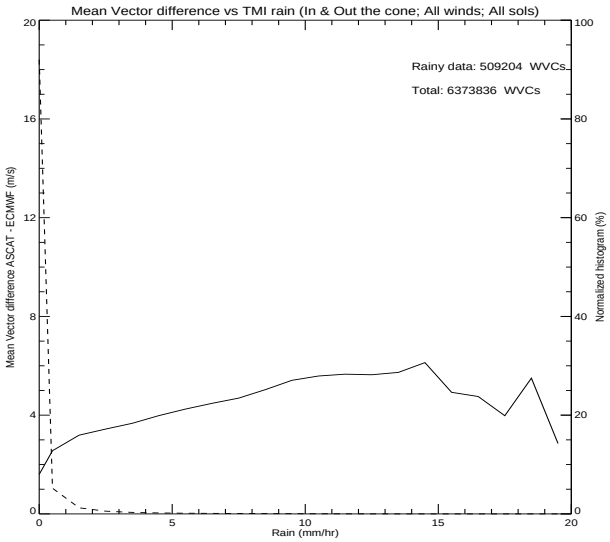

Figure 6. Mean VRMS difference between ASCAT and ECMWF winds as a function of TMI rain rate (bins of 1 mm/hr).

Figure 9 shows the same plots as Figure 8 but for a heavy rain case. Note that although the ASCAT QC rejects some of the WVCs under heavy rain (see yellow arrows around 6°N and 157°E, other WVCs are not (see central part of the wind field). The latter are clearly spatially inconsistent as denoted by the unrealistic patchiness of the wind arrows. This is an indication that the current ASCAT QC does not effectively remove heavy rain-contaminated WVCs. A more constrained QC threshold should be investigated to improve rain screening.

a)

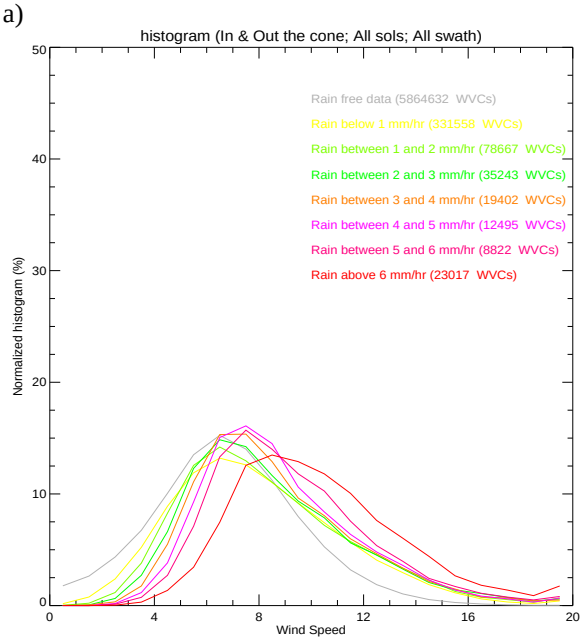

b)

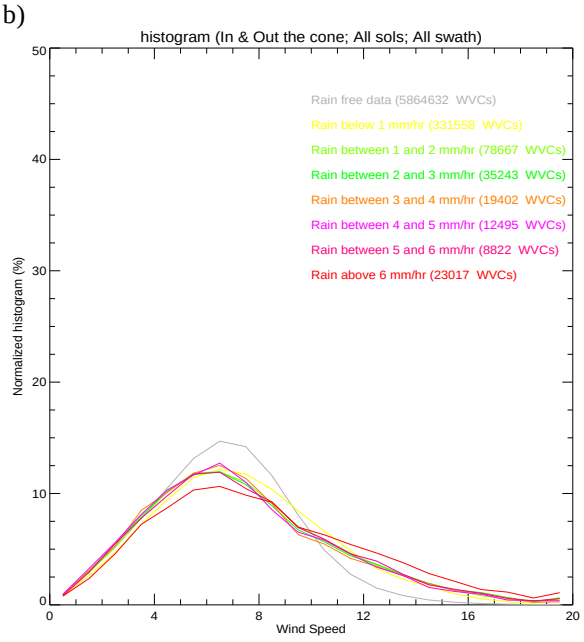

Figure 7. Wind speed histograms of both ASCAT (a) and ECMWF (b) winds for different TMI-derived RR intervals (see legend).

a)

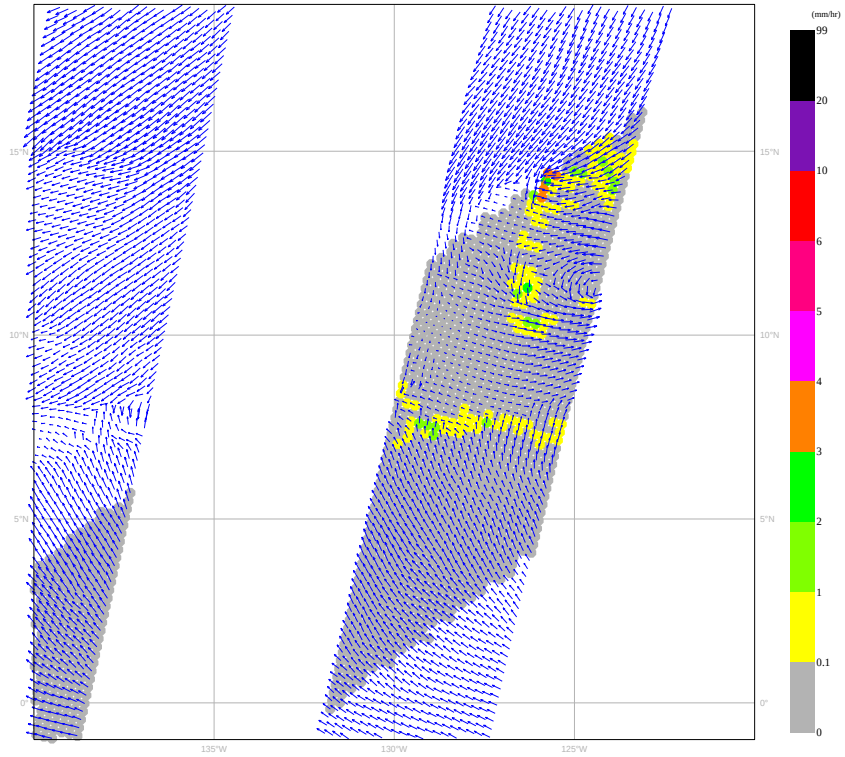

b)

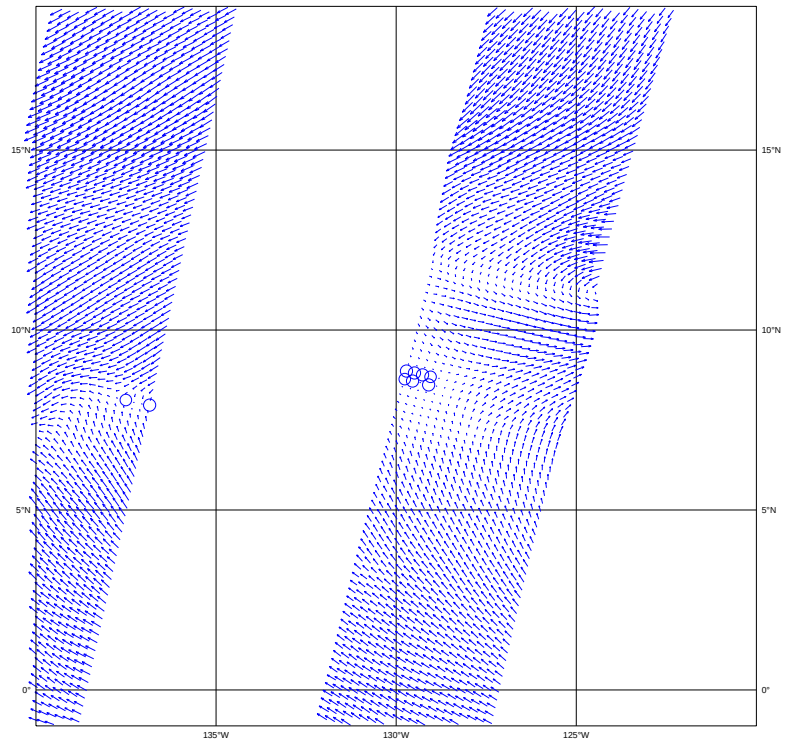

Figure 8. Collocated ASCAT-ECMWF-TMI data. (a) ASCAT wind arrows, where blue corresponds to accepted WVCs and yellow/orange to rejected WVCs. The colored areas superimposed correspond to different TMI rain rates (see legend). (b) Collocated ECMWF winds. The acquisition date was October 14 2008 at 17:42 UTC.

a)

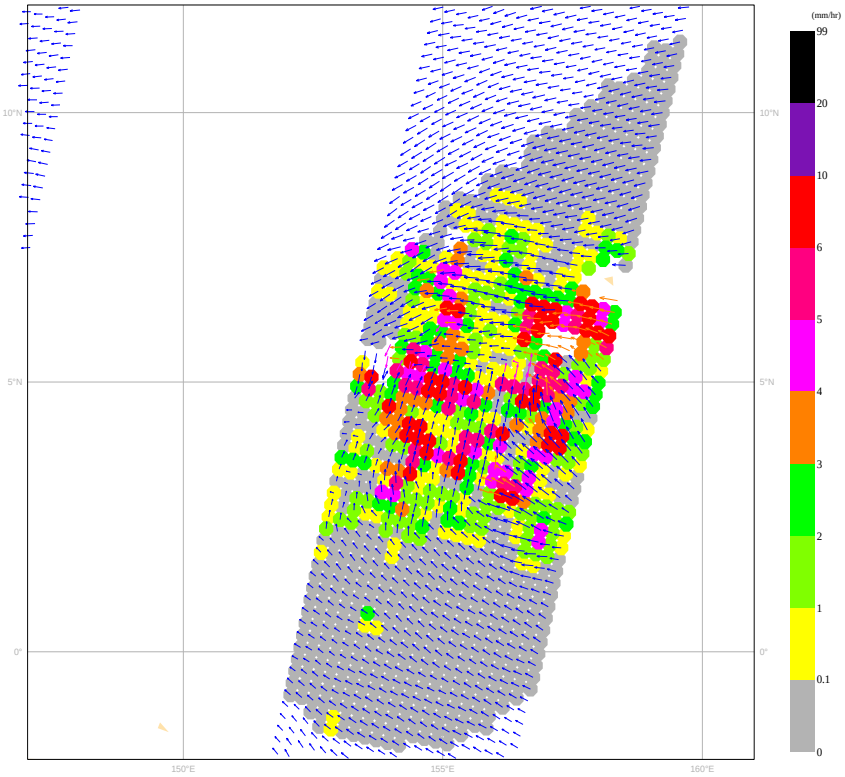

b)

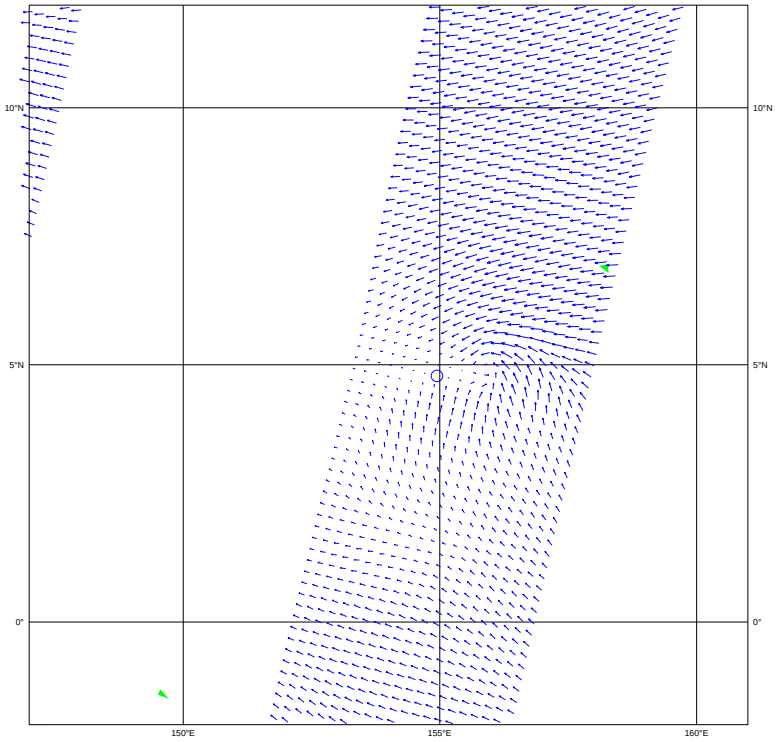

Figure 9. Same as Figure 8 but for October 14 2008 at 22:45 UTC and different location.

4 OUTLOOK

The ASCAT QC is improved by taking into account the MLE sign in addition to the MLE magnitude. Under light rain conditions, ASCAT derived winds appear to be of good quality whereas ECMWF winds seem to miss some rain-related effects. For RR above 6 mm/hr, ASCAT retrieved winds are clearly distorted by rain and should therefore be filtered out. Further improvements on ASCAT QC will focus on improving rain screening. The method proves to be very useful in further discriminating good wind quality cases from poor quality cases. This method is generic and opens the grounds for a more sophisticated QC for both past and future scatterometer missions.

The MLE analysis is also relevant in the context of a GMF improvement. A good GMF fit of the backscatter measurements should result in approximately the same amount of measurement triplets inside and outside the GMF cone surface. A careful analysis of the current C-band GMF, the so-called CMOD-5 [7], reveals that for low winds, the majority of triplets lie inside the cone, therefore indicating a GMF misfit. Furthermore, spatial patterns (i.e., maps) of the MLE sign are found to be correlated with sub-cell wind variability, indicating the potential sensitivity of scatterometer systems to the presence of, e.g., wind gust.

ACKNOWLEDGMENTS

The ASCAT level 1b data are provided by EUMETSAT. The software used in this work has been developed through the EUMETSAT Satellite Application Facilities (SAFs).

REFERENCES

1. Verspeek, J., Stoffelen, A., Portabella, M., Bonekamp, H., Anderson, C., and Figa Saldaña, J., (2010). Validation and calibration of ASCAT data using ocean backscatter and CMOD5.n. *IEEE Trans. Geosci. Rem. Sens.*, doi:10.1109/TGRS.2009.2027896, **48** (1), pp. 386-395.

2. Portabella, M., and Stoffelen, A. (2001). Rain detection and quality control of SeaWinds. *J. Atm. and Ocean Techn.*, ***18*** *(7)*, pp. 1171-1183.

3. Ebuchi, N., and Graber, H. C. (1998). Directivity of wind vectors derived from the ERS-1/AMI scatterometer. *J. Geophys. Res.*, vol. 103(C4), pp. 7787-7798.

4. Stoffelen, A., and Portabella, M. (2006). On Bayesian scatterometer wind inversion. *IEEE Trans. Geosci. Rem. Sens.*, **44** (6), doi:10.1109/TGRS.2005.862502, pp. 1523-1533.

5. Van De Hulst, H.C. (1957). Light Scattering by small particles. *John Wiley and Sons*, New York, pp. 428.

6. Boukabara, S.A., Hoffman, R.N., and Grassotti, C. (2000). Atmospheric Compensation and Heavy Rain Detection for SeaWinds Using AMSR. *Atmospheric Environmental Research Inc.*, 131 Hartwell Ave., Lexington, Massachussets (USA).

7. Hersbach, H., A. Stoffelen, and S. de Haan (2007). The improved C-band ocean geophysical model function: CMOD-5. *J. Geophys. Res.*, **112**, C03006, doi:10.1029/2006JC003743.